Supporting Information

Rational Design of Comb-Like 1D–1D ZnO–ZnSe Heterostructures Toward Its Excellent Performance on Flexible Photodetector

Ming-Jin Liu[#a, b, c], Hsuan-Chu Chen[#a, b, c], Tse-Ning Yang[a], Shu-Chi Wu[a, b, c], Yao-Jen Kuo[a, b, c], Ruei-Hong Cyu[a, b, c], Yu-Ren Peng[a, b, c], and Yu-Lun Chueh[a, b, c, d*]

[a] Department of Materials Science and Engineering, National Tsing-Hua University, 30013, Taiwan.

[b] College of Semiconductor Research, National Tsing-Hua University, Hsinchu, 30013, Taiwan

[c] Department of Physics, National Sun Yat-Sen University, Kaohsiung, 80424, Taiwan

[d] Department of Materials Science and Engineering, Korea University, Seoul 02841, Republic of Korea.

*E-mail: ylchueh@mx.nthu.edu.tw.

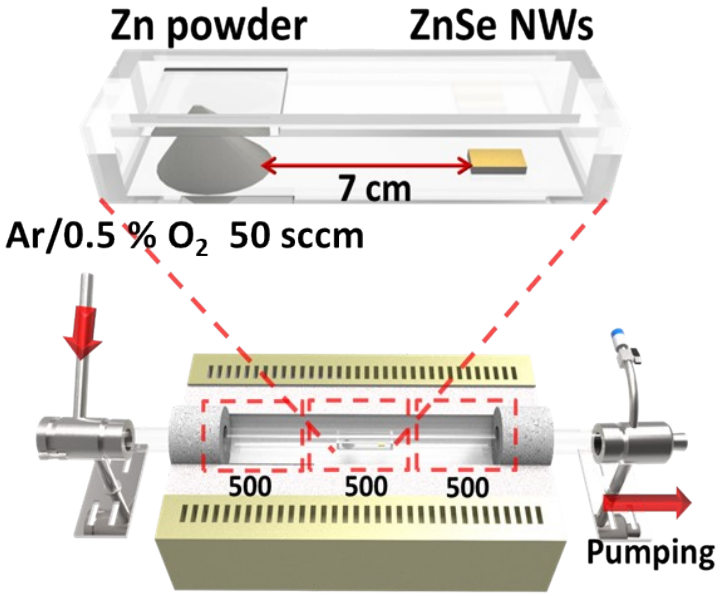

Figure S1 Schematic illustration of the growth process of the ZnO–ZnSe comb-like heterostructures

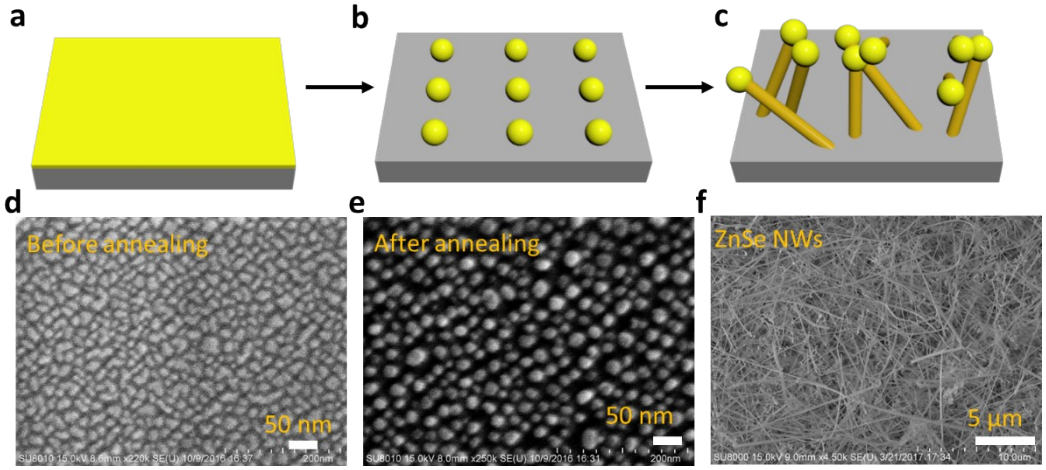

Figure S2 (a–c) Schematic procedures of ZnSe NWS by the VLS method. (a) An Au film was deposited on a Si substrate by electron beam evaporation. (b) The Au film was annealed at 600 °C under Ar gas flow rate of 100 sccm. (c) ZnSe NWs was obtained on the substrate. (d–e) SEM images of the Au film before and after the annealing process. (f) SEM images of ZnSe NWs grown on the Si substrate.

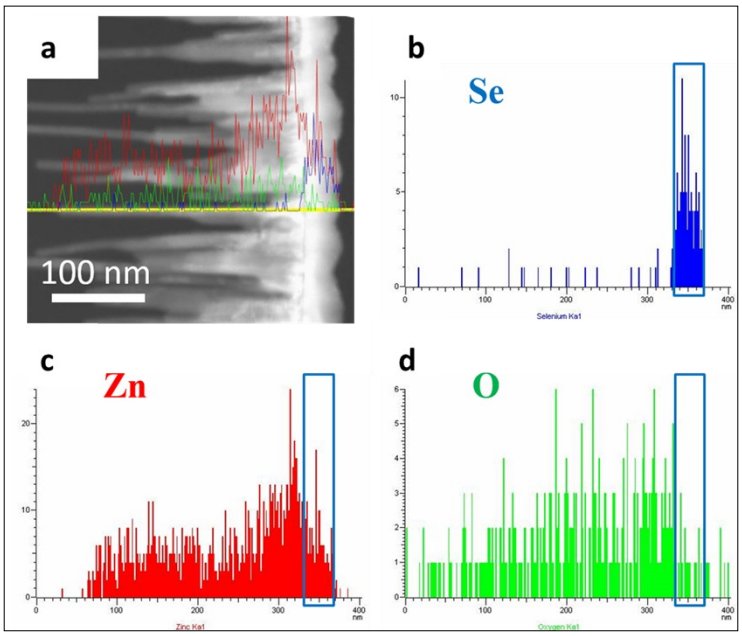

Figure S3 (a) The STEM image of ZnO–ZnSe NWs. EDS line profiles of the selected yellow line. Elemental distributions of (b) Se (c) Zn and (d) O, respectively

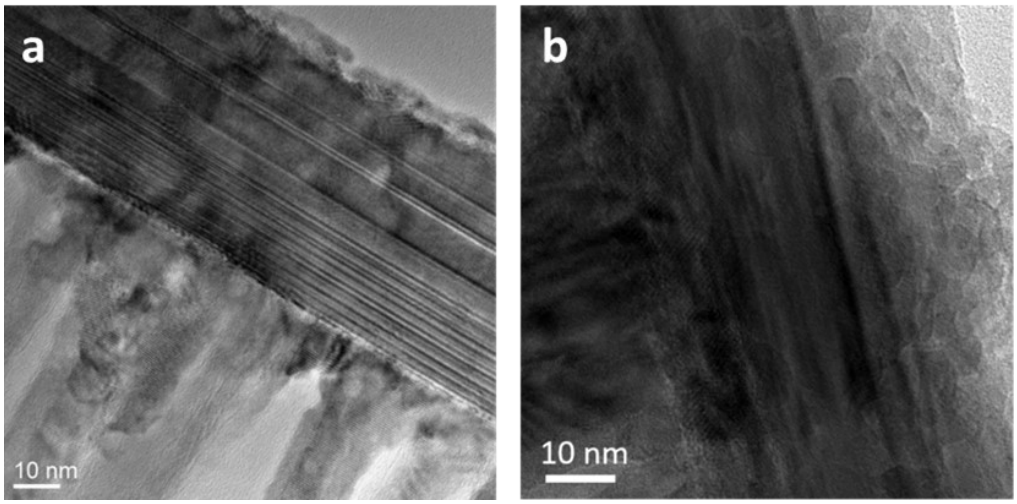

Figure S4. TEM images of the polycrystalline ZnO shells grown on the inverse side of ZnSe NWs

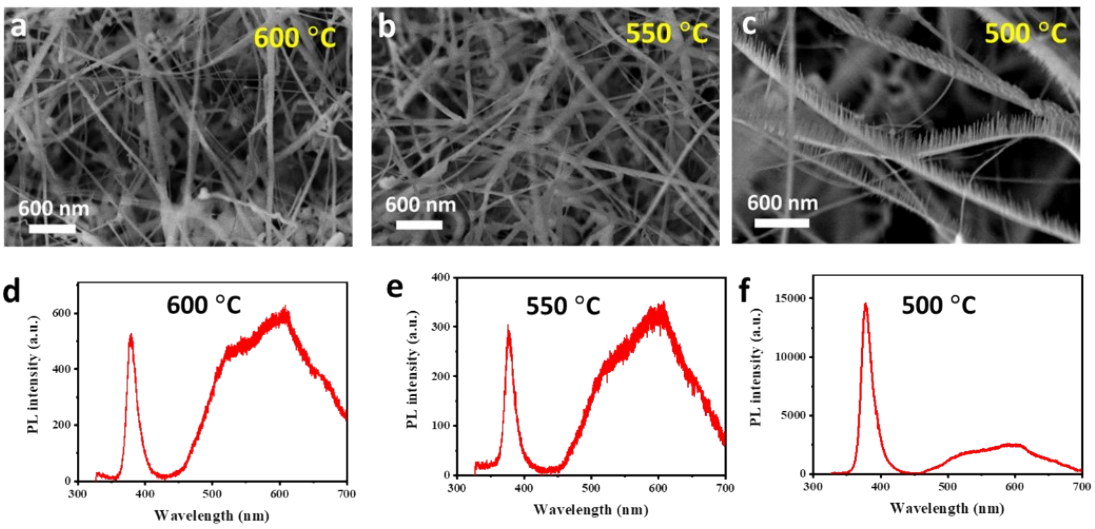

Figure S5 (a–c) SEM images of ZnO–ZnSe NWs prepared at 600, 550, and 500 °C, respectively. (d–f) PL spectra of the ZnO–ZnSe NWs prepared at 600, 550, and 500 °C, respectively. All these experiments were conducted at 20 torr for a duration of 10 minutes under Ar/0.5 % O_2 gas mixture flow rate of 50 sccm.

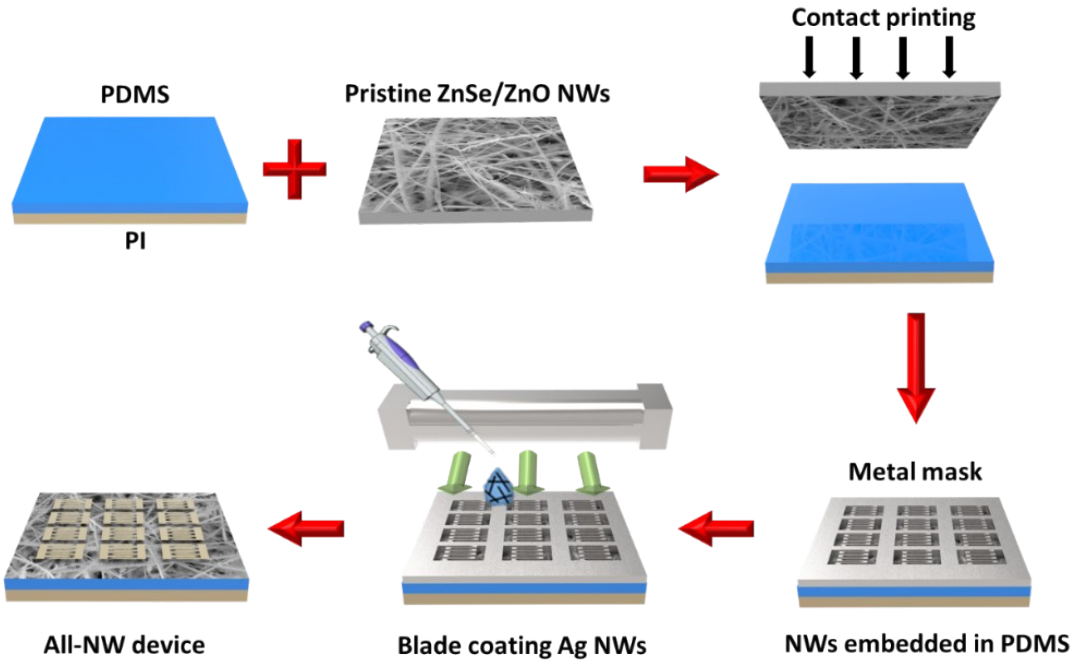

Figure S6 Schematics processes of the fabrication of ZnO–ZnSe NWs-based photodetector with Ag NWs as the electrode.

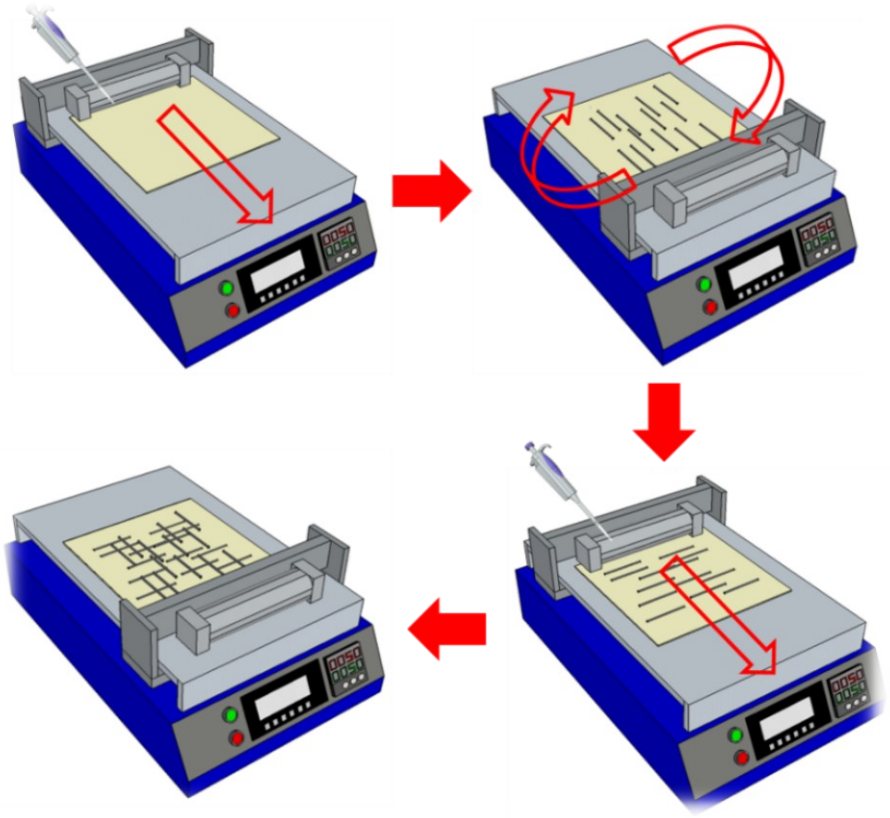

Figure S7. Schematic illustration of orthogonal coating Ag NWs networks via a commercial blade coating machine

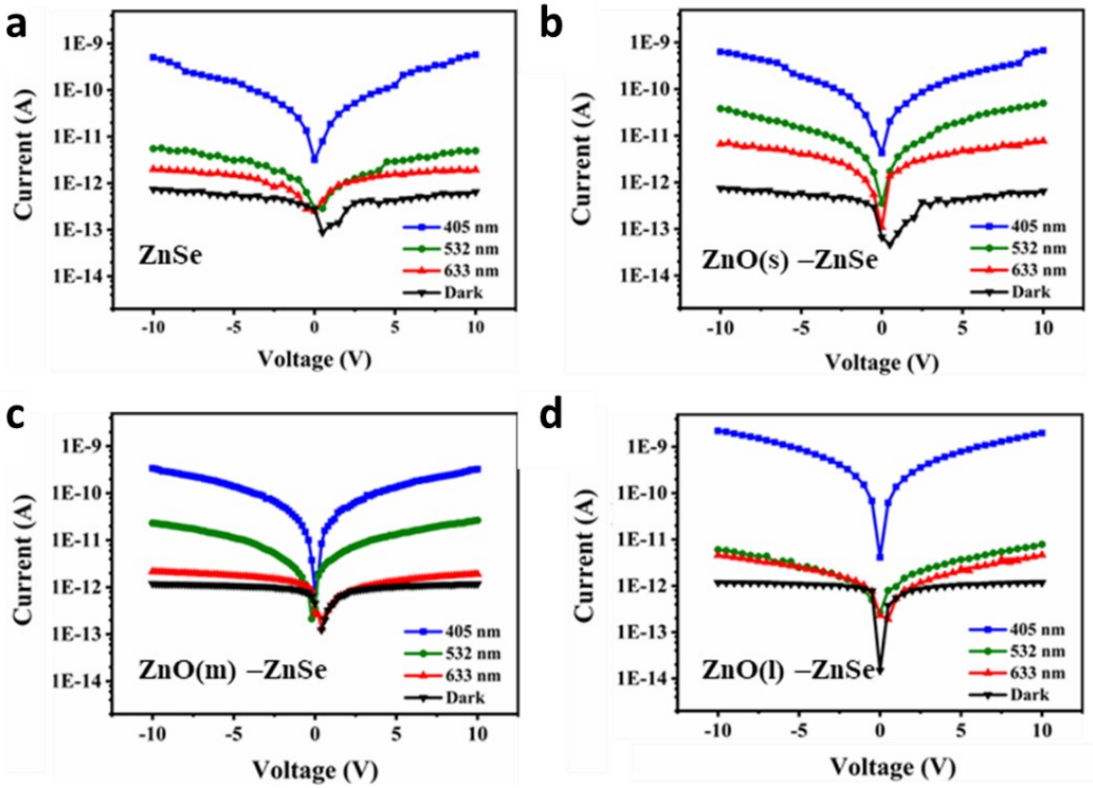

Figure S8 I-V characteristics of the (a) ZnSe, (b) ZnO(s)–ZnSe, (c) ZnO(m)–ZnSe, and (d) ZnO(l)–ZnSe devices under light illumination of 405, 532, 633 nm, and dark conditions, respectively.

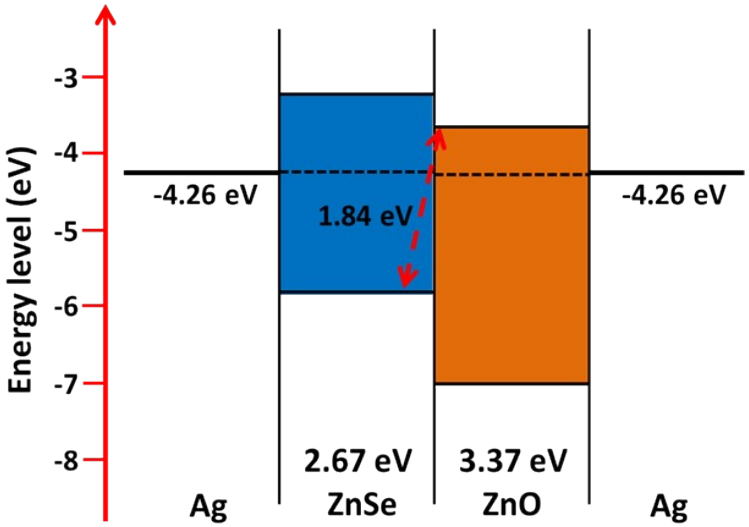

Figure S9 Thermal equilibrium band diagram of the ZnO–ZnSe heterostructure.

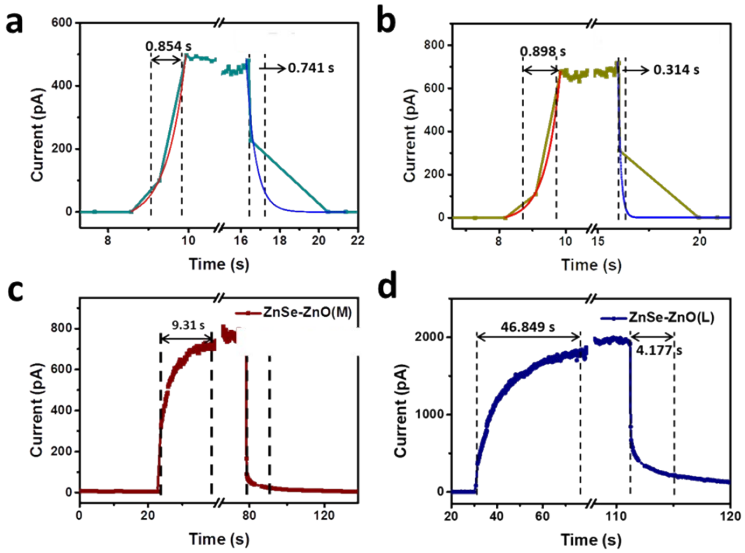

Figure S10 Time responses of (a) ZnSe, (b) ZnO(s)–ZnSe, (c) ZnO(m)–ZnSe, and (d) ZnO(l)–ZnSe NWs-based devices under blue light illumination of 405 nm at 10 V.